Surface-Based Integral Equation Formulations for Multiple Material and Conducting Objects

Vikram Jandhyala and Swagato Chakraborty
Applied Computational Electromagnetics Laboratory
Dept. of Electrical Engineering, University of Washington
jandhyala@ee.washington.edu

1. Introduction

The three basic computational approaches that are on the forefront of computational electromagnetics (CEM) are the finite element method (FEM), the finite difference time domain (FDTD) technique, and the method of moments (MoM). The first two techniques, based primarily on the partial differential equation (PDE) form of Maxwell's equations are powerful, reliable, and versatile techniques that are in general use for a variety of EM problems. These are not discussed or summarized in this tutorial except to briefly mention distinctions from the MoM approach.

MoM techniques are based on integral equation (IE) representation of fields and waves derived from Maxwell's equations. These methods have also been in use for several decades now. Unlike FEM and FDTD techniques, which lead to sparse matrices and matrix-free time-stepping respectively, the MoM approach leads to dense matrices based on Green's function interactions.

The MoM is also distinct from the FEM and FDTD in other ways, which can make it particularly suitable for certain classes of EM problems. The MoM in surface formulations only requires discretization of and unknowns placed on surfaces of homogeneous scatterers. This is contrast to PDE based methods where all space including the interior and exterior of scatterers are modeled. Furthermore, these PDE techniques also require truncation of the resulting grids or meshes through artificial absorbing boundary conditions (ABCs).

MoM techniques, in their complete generality, can be used with both volumetric IE formulations and surface IE formulations. This article concentrates on the use of MoM for surface IE formulations, wherein most of the advantages of the MoM are to be found. This tutorial is based on extensive work performed by several outstanding researchers over several decades, and no novelty of treatment is claimed in this article. One of the basic aim of the tutorial is to legitimize the use of surface-based techniques amongst simulation and design engineers who may be more attuned to volumetric techniques where conduction current is an easily understood physical quantity.

We will start with a review of the surface equivalence principle, which is the basic EM principle that enables surface-based IE formulations and resulting MoM. The ideal case of perfect conductors will be discussed as a simple version of this principle. The problem of modeling materials will be then summarized, and extended to multiple finite scatterers.

The important case of lossy conductors, particularly relevant to the microelectronics and emerging nanoelectronics regimes, will be discussed. In addition, a discussion of surface impedance approximations will follow. Finally, results and a discussion will be presented.

It should be pointed that no claim of completeness or wholeness of review is made. The article is based on the authors' necessarily limited viewpoints and experiences, and only supporting and relevant references are provided. Many of the cited works in turn refer to other excellent papers that may not necessarily be cited in this work itself, in addition to other important papers that exist in the extant literature as well.

The MoM formulations presented in this tutorial are implemented using the popular Rao-Wilton-Glisson basis functions. While several advances have been made in higher-order, hierarchical, and other basis functions, these are not in the scope of this article.

2. The Surface Equivalence Principle

Surface MoM-based solution of IE forms of Maxwell's Equations are typically based on the surface equivalence principle. This is an important mathematical principle, the existence of which is critical for the correct and exact formulation of MoMs. While this will be discussed again when discussing lossy conductors, it is important to note at the outset that the equivalent surface quantities produced by the application of this principle, and in particular the equivalent surface current, *may not necessarily have a physical meaning such as current flowing on or near a surface*. However, as will be shown, all relevant quantities including, if required, *volumetric conduction current*, can be accurately and exactly recovered, within mesh discretization and related solution error, from post-processing of the MoM system.

We will start with the case of a single homogeneous object (Region 2, with constitutive parameters ε_2 and μ_2) in a (different) homogeneous object (Region 1, with constitutive parameters ε_1 and μ_1). Without loss of generality, it is assumed that the scatterer is excited by a source in Region 1, as shown in Figure 1. The source and its interaction with the scatterer leads to *total* fields $\mathbf{E}_1$ and $\mathbf{H}_1$ in Region 1, and $\mathbf{E}_2$ and $\mathbf{H}_2$ in Region 2. The

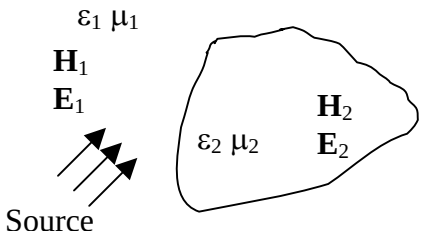

Figure 1: A homogeneous scatterer in a homogeneous medium, excited by an exterior source.

application of the surface equivalence principle in this instance proceeds as follows.

The original problem depicted in Figure 1 is replaced by two *equivalent* problems; the simultaneous solution of these two problems results in the same solution as that of the original problem, in the following sense. As shown in Figure 2, the equivalent exterior problem is constructed by replacing the scatterer by a *mathematical surface* of the same shape, shown with a dotted line. In addition, the entire space interior and exterior to the surface is filled with homogeneous material with constitutive parameters of the original background. It is assumed that in this problem, the correct total fields are produced in the Region 1 exterior to the mathematical surface, and that *zero* fields are produced inside Region 2. Therefore, there are discontinuities of fields across the surface. In order to support this jump, there must exist non-zero electric and magnetic current densities, tangential to the surface, $\mathbf{J}_1$ and $\mathbf{K}_1$. It is important to note that no *physical* meaning should be ascribed to these equivalent current densities; these are merely related to the tangential discontinuities of the fields produced by the mathematical specification of this equivalent problem, through the regular tangential boundary conditions for electric and magnetic fields. In Figure 2, $\hat{\mathbf{n}}$ represents the outward normal to the surface at any point. Note again that there is no object in this equivalent problem, only a mathematical surface on which exist equivalent current densities, which radiate into a completely homogeneous space. Also note that the original source is present.

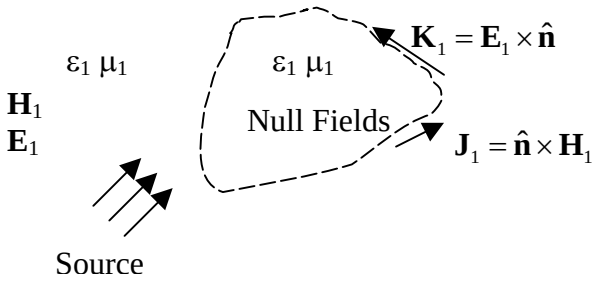

Figure 2: Equivalent exterior problem, with equivalent sources producing the correct total external fields and zero fields interior to the surface bounding the original Region 1.

The second equivalent problem, depicted in Figure 3, is the interior problem. In this case, the entire space is filled with the constitutive parameters of the scatterer.

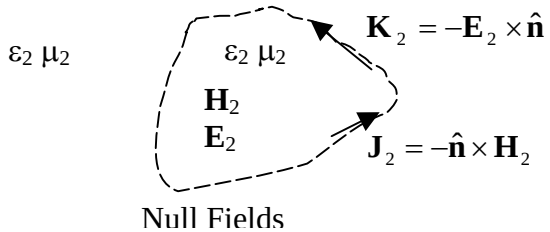

Figure 3: Equivalent interior problem, with equivalent sources producing the correct total internal fields and zero fields exterior to the surface bounding the original Region 1.

In this problem, it is assumed that equivalent current densities $\mathbf{J}_2$ and $\mathbf{K}_2$ which support a different discontinuity in the fields across the surface are produced. True fields are produced in the interior of the surface, and zero fields are produced outside. The original source no longer exists in this equivalent problem; however the current densities act as secondary sources producing non-zero fields inside the surface. Also note again that these are equivalent current densities only, not to be ascribed physical meaning, and that there is no object remaining in this problem, only a homogeneous medium.

The two equivalent problems are linked by the fact that the two sets of equivalent currents, $\mathbf{J}_1, \mathbf{K}_1$ and $\mathbf{J}_2, \mathbf{K}_2$ are not independent. In Figure 1, if tangentially boundary conditions are enforced across the scatterer surface, one can see that since there are no explicit electric or current source densities, the tangential fields must be continuous. Therefore, from the fact that each of the two equivalent problems generates the true fields on each side of the surface, that the two sets of currents must themselves be equal and opposite i.e. $\mathbf{J}_1 = -\mathbf{J}_2$ and $\mathbf{K}_1 = -\mathbf{K}_2$ so that the *true* boundary conditions $\hat{\mathbf{n}} \times (\mathbf{H}_1 - \mathbf{H}_2) = 0$ and $\hat{\mathbf{n}} \times (\mathbf{E}_1 - \mathbf{E}_2) = 0$ are enforced. Therefore the two equivalent problems need to be setup and solved simultaneously.

In Figures 2 and 3, it can be seen that the equivalent current densities in the exterior problem are shown to be on the outer side of the equivalent surface, and those in the interior problem are shown to be on the inner side of the surface. These limits can, in terms of limits of singular Green's function integrals as observation points approach the surface from either side, give rise to sign changes in formulations and are therefore important. Also, the fact that the equivalent currents produce null fields in the interior (for the equivalent exterior problem), and in the exterior (for the equivalent interior problem) can be used as a verification of correctness, or degree of accuracy, in MoM implementations. This fact (equivalent currents producing null fields) is termed the extinction theorem.

For the special case of a perfect electric conductor (PEC), which is an ideality that proves to be a useful approximation in several scattering problems, the equivalent problem becomes simpler as shown in Figures 4-6.

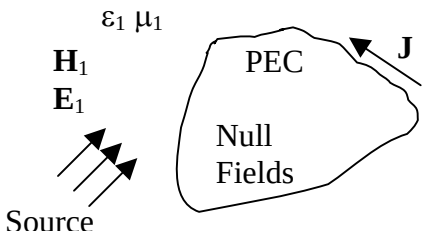

Figure 4: A PEC scatterer

The original scattering situation is shown in Figure 4. There are no fields produced inside the PEC. Also, a true surface current **J** is induced by the source. This current is an actual surface conduction current that exists on an ideal PEC. In addition, the boundary condition that the tangential electric field vanishes on the surface of a PEC needs to be considered. The exterior problem is shown in Fig. 5. Note that all the fields produced by the equivalent source $\mathbf{J}_1$ are the same as the true fields in Figure 4, including the null fields inside the PEC object of Figure 4. This current radiates in a homogeneous medium with constitutive parameters of Region 1. In this case the equivalent current is identical to the original surface current density **J**; and the original problem is simply replaced by one where the PEC object is replaced by its surface on which resides the current to be found.

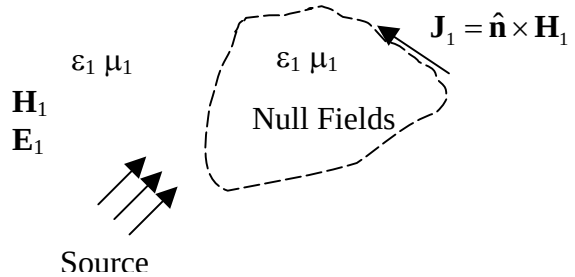

Figure 5: Equivalent exterior problem.

What about the interior equivalent problem ? This is shown in Figure 6. This is a *don't care* problem; no current can radiate in a complete PEC background, and hence there is no associated equation to setup or solve.

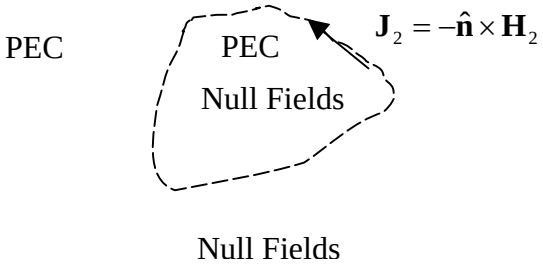

Figure 6: Equivalent interior problem. No radiation occurs in a homogeneous PEC environment.

Note that there are also no equivalent magnetic currents; the fact that the electric field has zero tangential component on the surface of the PEC assures this in the non-trivial exterior problem.

If the PEC is replaced by a finite conductivity metal structure, the exact equivalent problems are significantly different from the PEC case, and resemble the dielectric problem. Figure 7 shows the conductor of conductivity σ and the external source.

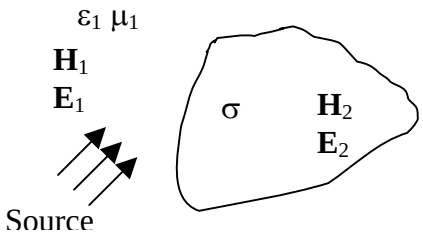

Figure 7: A homogeneous conducting scatterer in a homogeneous medium, excited by an exterior source.

In this case, in the exact formulation, both the exterior and interior problems, shown in Figures 8 and 9 are relevant.

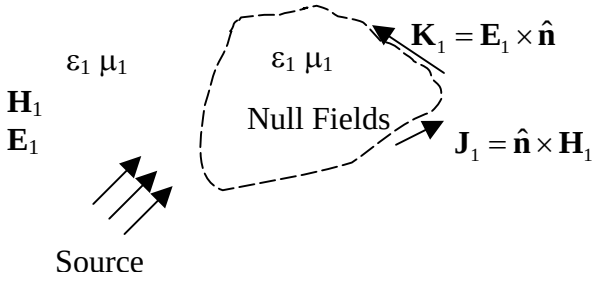

Figure 8: Equivalent exterior problem.

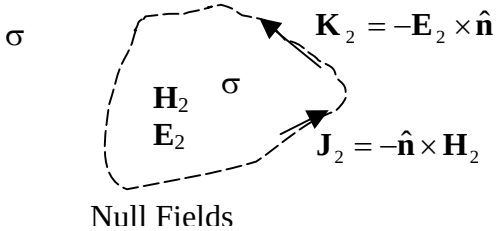

Figure 9: Equivalent interior problem. Currents radiate in a homogeneous region with the conducitivity of the original scatterer

In the interior problem, the homogenous material has finite conductivity and is therefore lossy but permits some propagation of fields. As the conductivity increases, this propagation will reduce, and it can be shown that the magnitude of the magnetic current density will drop. The case of finite conductivity will be discussed in more detail later in this paper. Note that unlike the PEC case, the fields interior to the conductor are not assumed to be zero, and that both electric and magnetic current densities are assumed, with no physical properties assigned to these quantities.

Finally, we will now generalize the discussion to an arbitrary number of material objects. If there are *N* such objects, there will be *N+1* simultaneous equivalent problems. The four equivalent problems for this case are shown in Figures 10-14.

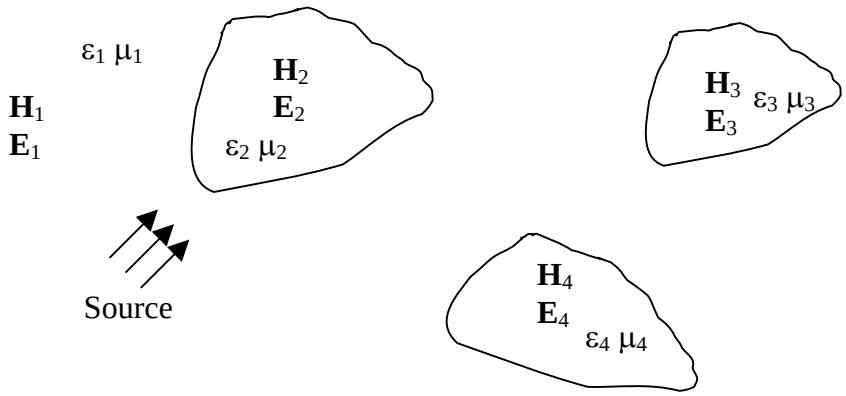

Figure 10: Original multibody problem.

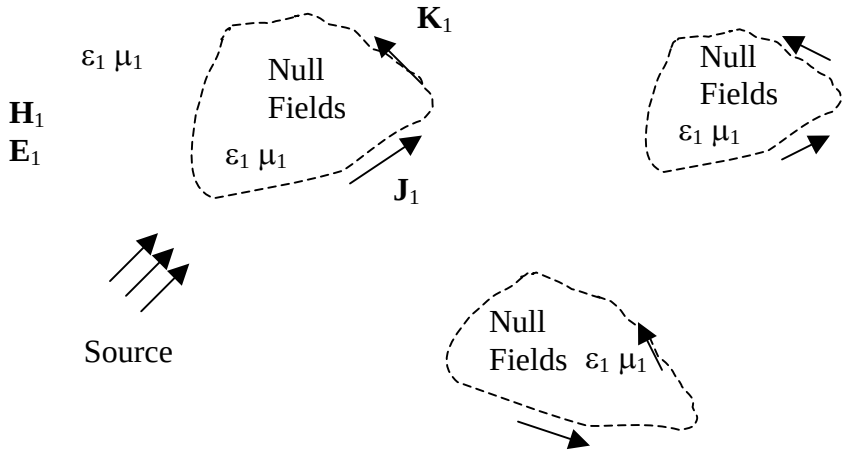

Figure 11: Equivalent problem for Region 1

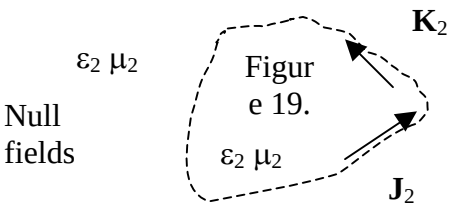

Figure 12: Equivalent problem for Region 2

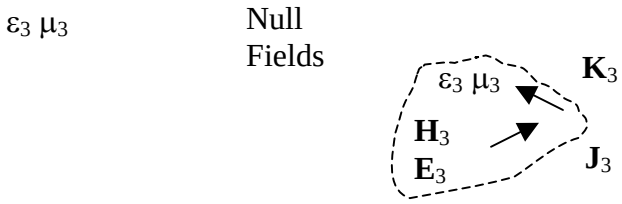

Figure 13: Equivalent problem for Region 3

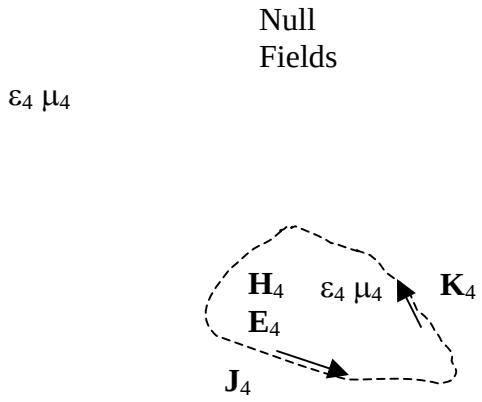

Figure 14: Equivalent problem for Region 4

From Figures 10-14, it is seen that the first equivalent problem includes all surfaces, and equivalent currents are placed on all of them. All the remaining equivalent problems have only one surface associated with them. As in the simpler cases, all these equivalent currents are not independent; they are equal and opposite to the equivalent currents in Figure 10 for each particular surface.

If any of the objects are conducting, the discussion on modeling finite conductivity objects is immediately valid. If any object is a PEC, the interior problem for that object is trivial and can be removed, and no magnetic currents are associated with that surface either in its own equivalent problem or in the first equivalent problem.

3. Surface Integral Equations for PEC Scatterers

3.1 Electric Field Integral Equation (EFIE)

The integral equations associated with a PEC scatterer are based on the exterior problem depicted in Figure 5. The total electric field in Region 1 satisfies the boundary condition

$$\mathbf{E}_1(\mathbf{r})\big|_{\tan} = 0\,,\ \mathbf{r} \in S \tag{1}$$

where *S* denotes the surface of the PEC scatterer, *tan* represents field quantities tangential to *S*, and $\mathbf{r}$ represents field observation points. If we split the field into an incident part created by the source and a scattered part created by the source interacting with the scatterer through the induced current **J,** we get the condition

$$\mathbf{E}_1{}^{scat}(\mathbf{r})\Big|_{\tan} + \mathbf{E}_1{}^{inc}(\mathbf{r})\Big|_{\tan} = 0 \tag{2}$$

where the scattered field is represented in mixed potential form as

$$\mathbf{E}_1{}^{scat}(\mathbf{r}) = -j\omega\mathbf{A}_1(\mathbf{r}) - \nabla\phi_1(\mathbf{r}) \tag{3}$$

where ω is the angular frequency, $\mathbf{A}$ and ϕ are the magnetic vector potential and electric scalar potential respectively and are obtained by convolution of the Green's function and sources, namely the surface current density $\mathbf{J}$ and the surface charge density ρ.

$$\mathbf{A}_1(\mathbf{r}) = \frac{\mu_1}{4\pi}\int_{S'} G_1(\mathbf{r},\mathbf{r}')\,\mathbf{J}_1(\mathbf{r}')\,ds' \tag{4}$$

$$\phi_1(\mathbf{r}) = \frac{1}{4\pi\varepsilon_1}\int_{S'} G_1(\mathbf{r},\mathbf{r}')\rho_1(\mathbf{r}')\,ds' \tag{5}$$

The Green's function is expressed as follows

$$G_1(\mathbf{r},\mathbf{r}') = \frac{e^{-jk_1|\mathbf{r}-\mathbf{r}'|}}{|\mathbf{r}-\mathbf{r}'|} \tag{6}$$

where k is the wave number in the corresponding medium and $\mathbf{r}$, $\mathbf{r}'$ are the observation and source points respectively. The surface charge density and the surface current density are related by the continuity equation given by

$$\nabla_S \cdot \mathbf{J}(\mathbf{r}) + j\omega\rho(\mathbf{r}) = 0 \tag{7}$$

Putting (7) in (5) we can write (3) as

$$-j\omega\frac{\mu_1}{4\pi}\int_{\mathbf{r}'\in S} G_1(\mathbf{r},\mathbf{r}')\mathbf{J}_1(\mathbf{r}')ds' - \nabla\frac{j}{4\pi\varepsilon_1\omega}\int_{\mathbf{r}'\in S} G_1(\mathbf{r},\mathbf{r}')(\nabla'\cdot\mathbf{J}_1(\mathbf{r}'))ds'\Big|_{\tan} = -\mathbf{E}_1{}^{inc}(\mathbf{r})\Big|_{\tan} \tag{8}$$

At this stage the unknown current density is discretized using basis functions $\mathbf{f}_i(\mathbf{r})$ scaled by unknown coefficients

$$\mathbf{J}(\mathbf{r}) = \sum_{i=1}^{N}\alpha_i\mathbf{f}_i(\mathbf{r}) \tag{9}$$

and we test (8) with a tangential testing function $\mathbf{t}(\mathbf{r})$ to obtain a system of linear equation given by

$$\overline{\mathbf{Z}}\,\mathbf{I} = \mathbf{V} \tag{10}$$

where ,

$$\begin{aligned} Z_{mn} = &\left\langle \mathbf{t}_m(\mathbf{r}), \left\{\frac{-j\omega\mu_1}{4\pi}\right\}\int_{\mathbf{r}_n'\in S_n} G_1(\mathbf{r},\mathbf{r}')\mathbf{f}_{1,n}(\mathbf{r}')ds'\right\rangle \\ &+\left\langle \nabla\cdot\mathbf{t}_m, \left\{\frac{j}{4\pi\varepsilon_1\omega}\right\}\int_{\mathbf{r}'\in S_n} G_1(\mathbf{r},\mathbf{r}')\nabla'\cdot\mathbf{f}_{1,n}(\mathbf{r}')ds'\right\rangle \end{aligned} \tag{11}$$

$$I_n = \alpha_n \tag{12}$$

$$V_m = \left\langle \mathbf{t}_m(\mathbf{r}), -\mathbf{E}_1{}^{inc}(\mathbf{r})\right\rangle \tag{13}$$

Typically, Rao-Wilton-Glisson based linear functions are used as both basis and testing functions, though higher order and curvilinear counterparts and multiresolution versions are now becoming increasingly widespread.

3.2 Magnetic Field Integral Equation (MFIE)

MFIE is an alternate approach for solving scattering problems where the boundary condition is enforced on the tangential magnetic field behavior across the PEC surface. The jump in the tangential magnetic field across the PEC boundary is supported by a surface current

$$\hat{\mathbf{n}}(\mathbf{r})\times\mathbf{H}_1(\mathbf{r}) - \hat{\mathbf{n}}(\mathbf{r})\times\mathbf{H}_2(\mathbf{r}) = \mathbf{J}_1(\mathbf{r}) \tag{14}$$

The magnetic field vanishes inside the PEC scatterer, and just outside the scatterer the total field is decomposed into an incident and scattered field as in (2)

$$\hat{\mathbf{n}}(\mathbf{r})\times\mathbf{H}_1{}^{inc}(\mathbf{r}) = \mathbf{J}_1(\mathbf{r}) - \hat{\mathbf{n}}(\mathbf{r})\times\mathbf{H}_1{}^{scat}(\mathbf{r}) \tag{15}$$

The scattered magnetic field is expressed in terms of magnetic vector potential as

$$\mathbf{H}_1{}^{scat}(\mathbf{r}) = \frac{1}{\mu_1}\nabla\times\mathbf{A}_1(\mathbf{r}) \tag{16}$$

Using (4), (15) and (16), and rearranging the order of the differential operator we get

$$\hat{\mathbf{n}}(\mathbf{r})\times\mathbf{H}_1{}^{inc}(\mathbf{r})=\frac{\mathbf{J}_1}{2}(\mathbf{r})+\hat{\mathbf{n}}(\mathbf{r})\times\frac{1}{4\pi\mu_1}\int_{\mathbf{r}'\in S}\nabla G_1(\mathbf{r},\mathbf{r}')\times\mathbf{J}_1(\mathbf{r}')ds' \tag{17}$$

Now expanding the unknown current density as in (9) and using the appropriate testing operation, we get a linear system similar to (10) , where the matrix elements are given by

$$Z_{mn}=\left\langle\mathbf{t}_m(\mathbf{r}),\frac{\mathbf{f}_{1,n}(\mathbf{r})}{2}\right\rangle+\left\langle\mathbf{t}_m(\mathbf{r}),\left(\hat{\mathbf{n}}(\mathbf{r})\times\frac{1}{4\pi\mu_1}\int_{\mathbf{r}'\in S_n}\nabla G_1(\mathbf{r},\mathbf{r}')\times\mathbf{f}_{1,n}(\mathbf{r}')ds'\right)\right\rangle \tag{18}$$

and the right hand side vector is

$$V_m=\left\langle\mathbf{t}_m(\mathbf{r}),-\hat{\mathbf{n}}\times\mathbf{H}_1{}^{inc}(\mathbf{r})\right\rangle \tag{19}$$

MFIE is an integral equation of second kind, hence has much better spectral properties and is more suitable for iterative solution. However applicability of MFIE is limited to closed 3D objects owing to the jump condition in the tangential boundary condition.

4. Surface Integral Equation for Penetrable Scatterers

4.1 Two-region PMCHWT

For non-PEC boundaries the tangential field components do not vanish on or inside the object enclosed by the surface. In that case the boundary conditions on the **E** and **H** fields are

$$\mathbf{E}_1\big|_{\tan}=\mathbf{E}_2\big|_{\tan} \tag{20a}$$

$$\mathbf{H}_1\big|_{\tan}=\mathbf{H}_2\big|_{\tan} \tag{20b}$$

To model such a problem, we use two equivalent problems, as discussed, the equivalent exterior problem (Fig. 8), and the interior equivalent problem (Fig. 9).
Decomposing the total field into the incident and the scattered field like (2) , (15) we get

$$\mathbf{E}_1^{scat}-\mathbf{E}_2^{scat}\Big|_{\tan}=-\mathbf{E}_1^{inc}+\mathbf{E}_2^{inc}\Big|_{\tan} \tag{21a}$$

$$\mathbf{H}_1^{scat}-\mathbf{H}_2^{scat}\Big|_{\tan}=-\mathbf{H}_1^{inc}+\mathbf{H}_2^{inc}\Big|_{\tan} \tag{21b}$$

Now we can express the field quantities in terms of the constituent potentials as follows

$$\left.\begin{aligned}&-j\omega\mathbf{A}_1(\mathbf{r},\mathbf{J}_1)-\nabla\phi_1\left(\mathbf{r},\frac{\nabla\cdot\mathbf{J}_1}{-j\omega}\right)-\frac{1}{\varepsilon_1}\nabla\times\mathbf{F}_1(\mathbf{r},\mathbf{K}_1)+\\&j\omega\mathbf{A}_2(\mathbf{r},\mathbf{K}_2)+\nabla\phi_2\left(\mathbf{r},\frac{\nabla\cdot\mathbf{J}_2}{-j\omega}\right)+\frac{1}{\varepsilon_2}\nabla\times\mathbf{F}_2(\mathbf{r},\mathbf{K}_2)\end{aligned}\right|_{\tan}=-\mathbf{E}_1^{inc}(\mathbf{r})+\mathbf{E}_2^{inc}(\mathbf{r})\Big|_{\tan} \tag{22a}$$

$$\left.\begin{aligned} &-j\omega\mathbf{F}_1(\mathbf{r},\mathbf{K}_1)-\nabla\psi_1\left(\mathbf{r},\frac{\nabla\cdot\mathbf{K}_1}{-j\omega}\right)+\frac{1}{\mu_1}\nabla\times\mathbf{A}_1(\mathbf{r},\mathbf{J}_1)+\\ &j\omega\mathbf{F}_2(\mathbf{r},\mathbf{K}_2)+\nabla\psi_2\left(\mathbf{r},\frac{\nabla\cdot\mathbf{K}_2}{-j\omega}\right)-\frac{1}{\mu_2}\nabla\times\mathbf{A}_2(\mathbf{r},\mathbf{J}_2)\end{aligned}\right|_{\tan} = -\mathbf{H}_1^{inc}(\mathbf{r})+\mathbf{H}_2^{inc}(\mathbf{r})\Big|_{\tan} \quad (22b)$$

Here the additional potential quantities, namely the electric vector potential **F,** and the magnetic scalar potential ψ are given in by the following expressions

$$\mathbf{F}_p(\mathbf{r},\mathbf{K}) = \frac{\varepsilon_p}{4\pi}\int_{\mathbf{r}\in S'} G_p(\mathbf{r},\mathbf{r}')\mathbf{K}_p(\mathbf{r}')ds' \quad (23a)$$

$$\psi_p\left(\mathbf{r},\frac{\nabla\cdot\mathbf{K}}{-j\omega}\right) = \frac{1}{4\pi\mu_p}\int_{\mathbf{r}\in S'} G_p(\mathbf{r},\mathbf{r}')\left(\frac{\nabla\cdot\mathbf{K}_p(\mathbf{r}')}{-j\omega}\right)ds' \quad (23b)$$

where the subscript *p* indicates the corresponding medium where the potential is computed. The source $\mathbf{K}_p$ is the equivalent surface magnetic current radiating in the region *p* as described in Fig. (8-9). The unknown electric and magnetic current densities in the interior and the exterior medium are related by a negative sign as discussed. Finally the unknown electric and magnetic surface current densities are expanded as

$$\mathbf{J}(\mathbf{r}) = \sum_{i=1}^{N}\alpha_i\mathbf{f}_i(\mathbf{r}) \quad (24a)$$

$$\mathbf{K}(\mathbf{r}) = \sum_{i=1}^{N}\beta_i\mathbf{f}_i(\mathbf{r}) \quad (24b)$$

Following the standard testing operation a linear system similar to (10) is constructed where

$$\overline{\mathbf{Z}} = \begin{pmatrix} \overline{\mathbf{L}}_{EJ} & \overline{\mathbf{M}}_{EK} \\ \overline{\mathbf{M}}_{HJ} & \overline{\mathbf{L}}_{HK} \end{pmatrix} \quad (25)$$

The sub-blocks are linear operators given by

$$\begin{aligned} L_{EJ\,mn} = {} & \frac{-j\omega}{4\pi}\left\langle \mathbf{t}_m(\mathbf{r}), \left\{ \mu_1 \int_{\mathbf{r}_n'\in S_n} G_1(\mathbf{r},\mathbf{r}')\mathbf{f}_{1,n}(\mathbf{r}') + \mu_2 \int_{\mathbf{r}_n'\in S_n} G_2(\mathbf{r},\mathbf{r}')\mathbf{f}_{1,n}(\mathbf{r}')ds' \right\} \right\rangle \\ & + \frac{j}{4\pi\omega}\left\langle \nabla\cdot\mathbf{t}_m, \left\{ \frac{1}{\varepsilon_1}\int_{\mathbf{r}'\in S_n} G_1(\mathbf{r},\mathbf{r}')\nabla'\cdot\mathbf{f}_{1,n}(\mathbf{r}')ds' + \frac{1}{\varepsilon_2}\int_{\mathbf{r}'\in S_n} G_2(\mathbf{r},\mathbf{r}')\nabla'\cdot\mathbf{f}_{1,n}(\mathbf{r}')ds' \right\} \right\rangle \end{aligned} \quad (26a)$$

$$\begin{aligned} L_{HK\,mn} = {} & \frac{-j\omega}{4\pi}\left\langle \mathbf{t}_m(\mathbf{r}), \left\{ \varepsilon_1 \int_{\mathbf{r}_n'\in S_n} G_1(\mathbf{r},\mathbf{r}')\mathbf{f}_{1,n}(\mathbf{r}') + \varepsilon_2 \int_{\mathbf{r}_n'\in S_n} G_2(\mathbf{r},\mathbf{r}')\mathbf{f}_{1,n}(\mathbf{r}')ds' \right\} \right\rangle \\ & + \frac{j}{4\pi\omega}\left\langle \nabla\cdot\mathbf{t}_m, \left\{ \frac{1}{\mu_1}\int_{\mathbf{r}'\in S_n} G_1(\mathbf{r},\mathbf{r}')\nabla'\cdot\mathbf{f}_{1,n}(\mathbf{r}') + \frac{1}{\mu_2}\int_{\mathbf{r}'\in S_n} G_2(\mathbf{r},\mathbf{r}')\nabla'\cdot\mathbf{f}_{1,n}(\mathbf{r}') \right\} ds' \right\rangle \end{aligned} \quad (26b)$$

$$M_{EK\,mn} = -\left\langle \frac{\mathbf{t}_m(\mathbf{r})}{4\pi}, \left\{ \frac{1}{\varepsilon_1} \int_{\mathbf{r}' \in S_n} \nabla G_1(\mathbf{r},\mathbf{r}') \times \mathbf{f}_{1,n}(\mathbf{r}')\, ds' + \frac{1}{\varepsilon_2} \int_{\mathbf{r}' \in S_n} \nabla G_1(\mathbf{r},\mathbf{r}') \times \mathbf{f}_{1,n}(\mathbf{r}')\, ds' \right\} \right\rangle \quad (26c)$$

$$M_{HJ\,mn} = \left\langle \frac{\mathbf{t}_m(\mathbf{r})}{4\pi}, \left\{ \frac{1}{\mu_1} \int_{\mathbf{r}' \in S_n} \nabla G_1(\mathbf{r},\mathbf{r}') \times \mathbf{f}_{1,n}(\mathbf{r}')\, ds' + \frac{1}{\mu_2} \int_{\mathbf{r}' \in S_n} \nabla G_1(\mathbf{r},\mathbf{r}') \times \mathbf{f}_{1,n}(\mathbf{r}')\, ds' \right\} \right\rangle \quad (26d)$$

The vector of unknowns is given as

$$\mathbf{I} = \begin{bmatrix} \alpha_n \\ \beta_n \end{bmatrix}, n = 1 \ldots N \quad (27)$$

,and the right hand side vector is

$$\mathbf{V} = \begin{bmatrix} \left\langle \mathbf{t}_m(\mathbf{r}), \left\{ -\mathbf{E}_1^{inc}(\mathbf{r}) + \mathbf{E}_2^{inc}(\mathbf{r}) \right\} \right\rangle \\ \left\langle \mathbf{t}_m(\mathbf{r}), \left\{ -\mathbf{H}_1^{inc}(\mathbf{r}) + \mathbf{H}_2^{inc}(\mathbf{r}) \right\} \right\rangle \end{bmatrix}, m = 1 \ldots N \quad (28)$$

Note that the size of the linear system doubles compared to the PEC problems, as the boundary conditions are on both the electric and the magnetic fields, and the unknowns are the electric and magnetic surface current densities.

4.2 Multi-region PMCHWT

The most general configuration consists of an arbitrary number of regions of materials, embedded in a background or free-space. These regions can intersect or touch in general. The approach is to use M+1 surface equivalent problems for M regions (and 1 background region). Then, appropriate boundary conditions (tangential E and H fields), and appropriate identification of independent currents are used to set up the overall equation. The following conditions are used to set up the equations:

•For an interface between a dielectric and a PEC region, the tangential electric field is zero, no equation is present for the tangential magnetic field, the exterior of the PEC has only electric current, and the interior of the PEC does not have any associated unknowns

•For an interface (regions i and j) between two dielectrics or poor conductors, $\mathbf{J}_i = -\mathbf{J}_j$, $\mathbf{K}_i = -\mathbf{K}_j$, $\mathbf{E}_i = \mathbf{E}_j$, and $\mathbf{H}_i = \mathbf{H}_j$

•For an interface between a dielectric and conductor, or between two dissimilar conductors, $\mathbf{J}_i = -\mathbf{J}_j$, and $\mathbf{E}_i = \mathbf{E}_j$

• Boundary conditions and dependence of the basis functions as described above enforced by a sparse, bipolar matrix $\mathbf{P}_{M \times N}$, where M is the number of independent basis functions and N is the number of all basis functions combining individual regions.

The system of linear equations thus obtained is presented by

$$\overline{\mathbf{P}}^T_{M \times N} \overline{\mathbf{Z}}_{N \times N} \overline{\mathbf{P}}_{N \times M} \mathbf{I}_M = \overline{\mathbf{P}}^T_{M \times N} \mathbf{V}_N \quad (29)$$

Where $\overline{\mathbf{Z}}$ is a region by region PMCHWT matrix similar to (25), except that the entries correspond only to a single region rather than the sum of the contributions from two regions.

Pictorially, the matrix equation can be represented as:

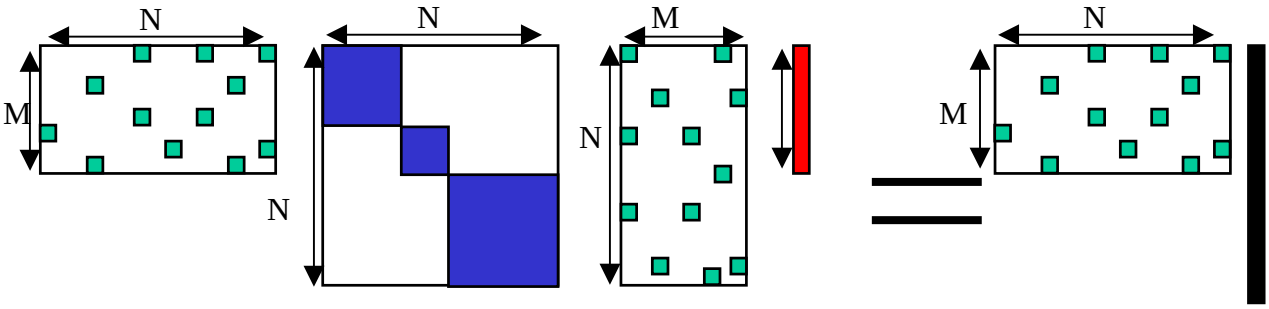

Figure 15: Pictorial representation of the multiregion PMCHWT system matrix

The Green elements are 1's or –1's, the rest of the rectangular matrix contains zeroes, the blue dense portion of the MoM matrix represents interactions within each region, using the Green's function for that region. The red vector is the set of independent electric and magnetic currents, and the long black vector is the set of incident fields.

It is important to take care of the junction problem while handling more than two touching dielectric regions. This is achieved by identify the independent basis function(s) corresponding to the junction and also to set up the corresponding $\overline{\mathbf{P}}$ matrix entries for the associated dependent basis functions. We do not discuss junctions in any detail here.

5. Surface Integral Equation for Lossy Scatterers

For boundary enclosing a region with finite conductivity, the tangential electric field does not vanish on the surface, hence there exists a magnetic current on the boundary and the problem can in general be modeled using PMCHWT equations as described in section 4. The wave number for a conducting medium is given by

$$k = \omega\sqrt{\mu\varepsilon_0\left(1+\frac{\sigma}{j\omega\varepsilon_0}\right)} \tag{30}$$

where σ is the conductivity of the region. For highly conducting regions, the wave number has a strongly negative imaginary part, so the corresponding Green's function (6) is associated with a very sharp decay which corresponds to the loss in the medium. When the decay becomes very sharp, i.e. for the case of very high conductivity and very high frequency the interior medium Green's function looks like a delta function, and in the limiting case the electric field contribution of the current in the interior medium can be represented locally by a linear term as

$$\mathbf{E}_2 = Z_S \mathbf{J}_2 = (1+j)\sqrt{\frac{\mu\omega}{2\sigma}}\mathbf{J}_2 \tag{31}$$

Z_S has been described in the literature as the surface impedance, and can be used to simplify the PMCHWT formulation using an impedance boundary condition (IBC) for the restricted case of high conductivity and high frequency. The IBC imposes a local relationship between the surface electric and magnetic current as

$$\mathbf{K} = -Z_S \hat{n} \times \mathbf{J} \tag{32}$$

However, as mentioned before the IBC is a simplification that is applied only to the cases involving high frequency and high conductivity. Whereas a complete two region PMCHWT formulation is general in terms of it applicability to lower frequencies and conductivities, and automatically reduces to IBC at higher frequencies. The Green's function convolution involving highly decaying kernels for conducting media can be handled using specially designed semi-analytic quadrature routines using polar coordinate system.

The surface based technique for modeling loss in conducting structures is useful to evaluate the actual volumetric current flow through the conductor cross-section. The system of linear equations as described in (25-28) is solved to obtain the distribution of equivalent electric and magnetic current on the conductor surface. The surface currents can be post-processed to find the true electric field distribution in the interior of the conductor using the interior medium Green's function as depicted in figure 9. Finally the true volumetric current inside the conducting region $\mathbf{J}_{vol}$ is obtained as

$$\mathbf{J}_{vol}(\mathbf{r}) = \sigma\, \mathbf{E}_2(\mathbf{r}) \tag{33}$$

where $\mathbf{E}_2$ is the interior medium electric field, computed using the interior medium material properties and the equivalent surface electric and magnetic current in the interior region.

The overall impact of such an approach is a purely surface formulation that correctly captures the volumetric effects including conduction current distribution.

6. Sample Results

Several excellent papers in the literature present exhaustive results using surface based PEC and dielectric MoM formulations. Here, we present some results related to the use of the surface MoM for conducting media, an approach that is occasionally misunderstood with the assumption that some surface approximation to the true conduction current is being enforced. As discussed in the previous sections, this is of course not true as explained through the surface equivalence principle, but this will also be shown through some examples.

Also, all examples shown here are produced using the PILOT code suite, an MoM-based code developed at the Applied Computational Electromagnetics Lab, University of Washington. This integrated code suite includes both surface and hybrid surface-volume formulations, special quadrature for lossy media, circuit interconnectivity and SPICE models, fast frequency sweeps, fast multilevel multipole and rank-compression

algorithms, and multi-stage loop-tree and approximate inverse preconditioners, with algorithms parallelized for multi-processor and workstation clusters.

The first example, in Figure 16 shows a Copper inductor of dimensions $200\,\mu m \times 200\,\mu m$ and metal width $20\,\mu m$ over a substrate of height $100\,\mu m$. The substrate has a conductivity of 1×10^5 S/m. The MoM code with lossy conductor modeling is used to obtain the quality factor of the inductor. The extremely low peak value of Q is typical of non-optimized on-chip inductors over lossy substrates, although the low Q is exaggerated here because of the high conductivity substrate.

The second example, in Figures 17 and 18, shows the extracted inductance and resistance of a Copper bar of dimension $0.5\text{mm}\times0.5\text{mm}\times5\text{mm}$, and conductivity $5.8\times10^7\,\text{Sm}^{-1}$. The limiting values of inductance at low and high frequency match against commercial solver, and the expected "S" shaped curve for inductance is obtained with the lossy medium, but not with a simplistic surface impedance approximation. For simple structures like a single bar, the quasi-static resistance can be computed analytically from the skin depth at a given frequency. The analytic resistance exhibits (Figure 18) a close match with the simulation result including the low frequency level-off to the DC resistance, *from a surface-only formulation*. For higher frequencies, the surface impedance results match with the PMCHWT results. However for lower frequencies, the surface impedance based model fails to capture the level-off of the resistance and the inductance curves, that arise due to uniform current flow through the conductor cross-section. The true lossy medium surface formulation captures all relevant resistance effects including near DC.

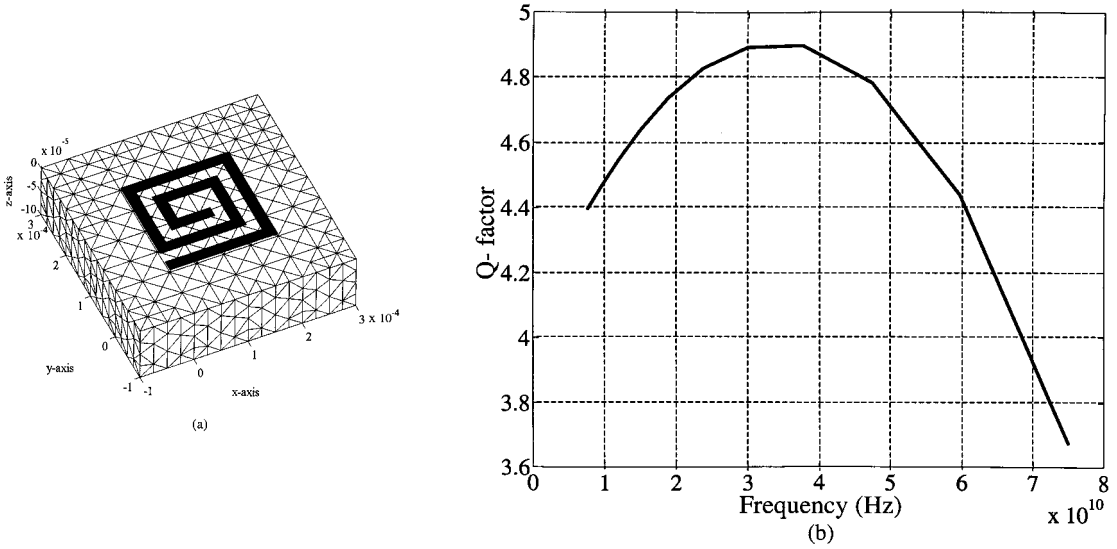

Figure 16: Quality factor of an on-chip spiral inductor on a conducting substrate.

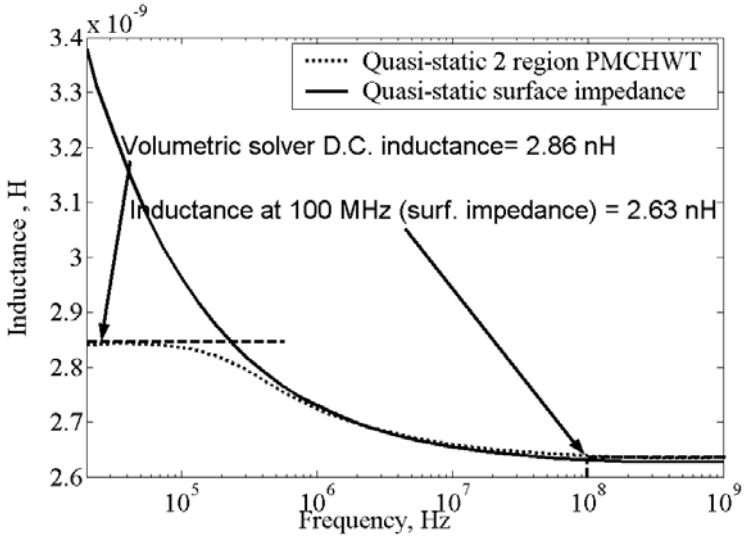

Figure 17: Frequency variation of inductance of a Copper bar using a lossy medium PMCHWT surface formulation

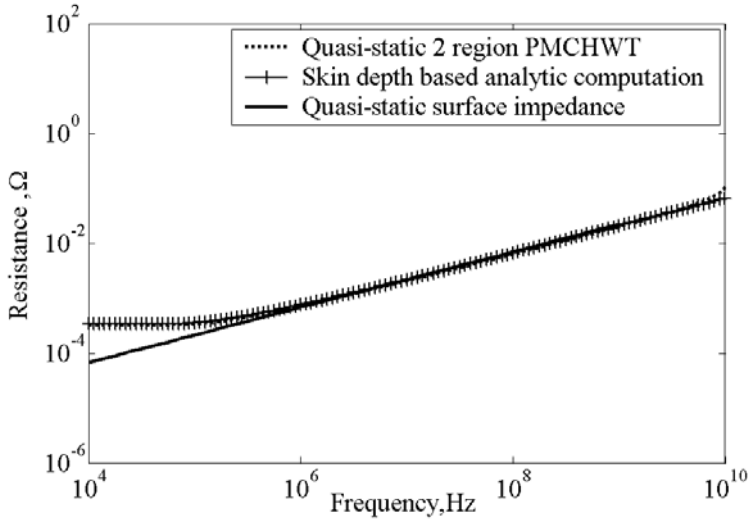

Figure 18: Frequency variation of resistance of a Copper bar using a lossy medium PMCHWT surface formulation.

The next example examines the volumetric current density within a metallic square cross section conductor, captured by post-processing fields obtained from a surface-only formulation. Increasing skin effect in a conductor can happen by changing frequency or conductivity. The case of changing conductivity is shown; as conductivity is increased, the volumetric current attempts to flow near the surface. The same effect can also be shown by plotting, on a log-scale, the fall off of volumetric current away from the surface of the conductor. The numerical value obtained from the surface formulation compares

favorably to the drop-off predicted by an analytic skin-depth approximation, as shown in Figure 20.

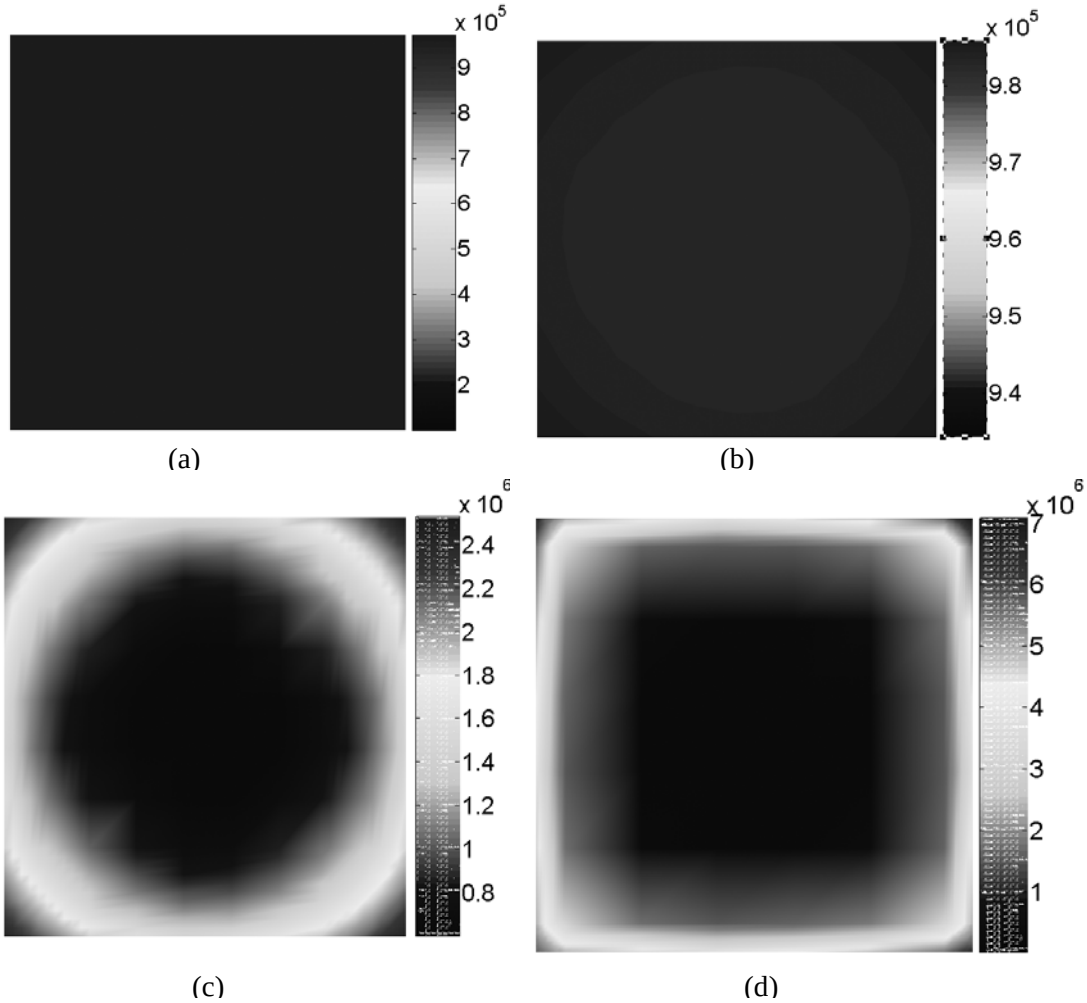

Figure 19. Current distribution in the cross section of a square conductor, with the following ratios of minimum to maximum volumetric current for given conductivities

(a) $\frac{J_{\min}}{J_{\max}} = 0.99,\ freq. = 1MHz, \sigma = 5.8\times10^{4}$

(b) $\frac{J_{\min}}{J_{\max}} = 0.52,\ freq. = 1MHz, \sigma = 5.8\times10^{5}$

(c) $\frac{J_{\min}}{J_{\max}} = 0.1037,\ freq. = 1MHz, \sigma = 5.8\times10^{6}$

(d) $\frac{J_{\min}}{J_{\max}} = 0.0009,\ freq. = 1MHz, \sigma = 5.8\times10^{7}$

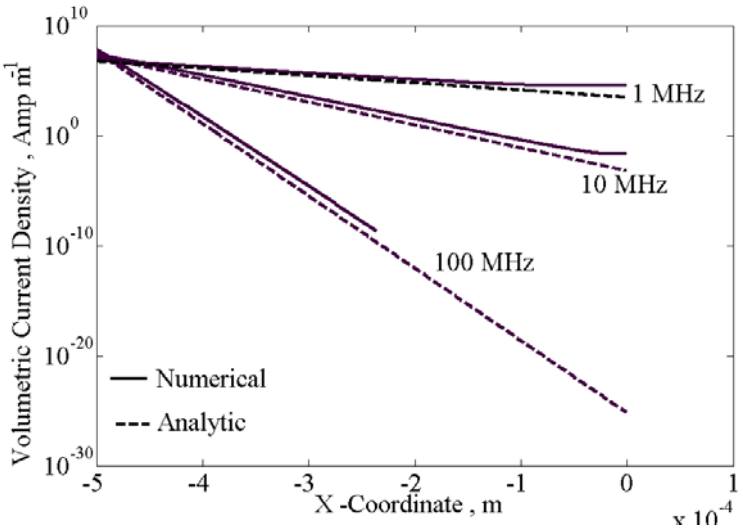

Figure 20. Variation of volumetric current density with the distance from the surface ($x = -0.5mm$) of a copper conductor with uniform cross section of $1mm \times 1mm$. The rate of decay is compared against the rate computed from the analytic expression of skin depth for a given frequency and conductivity.

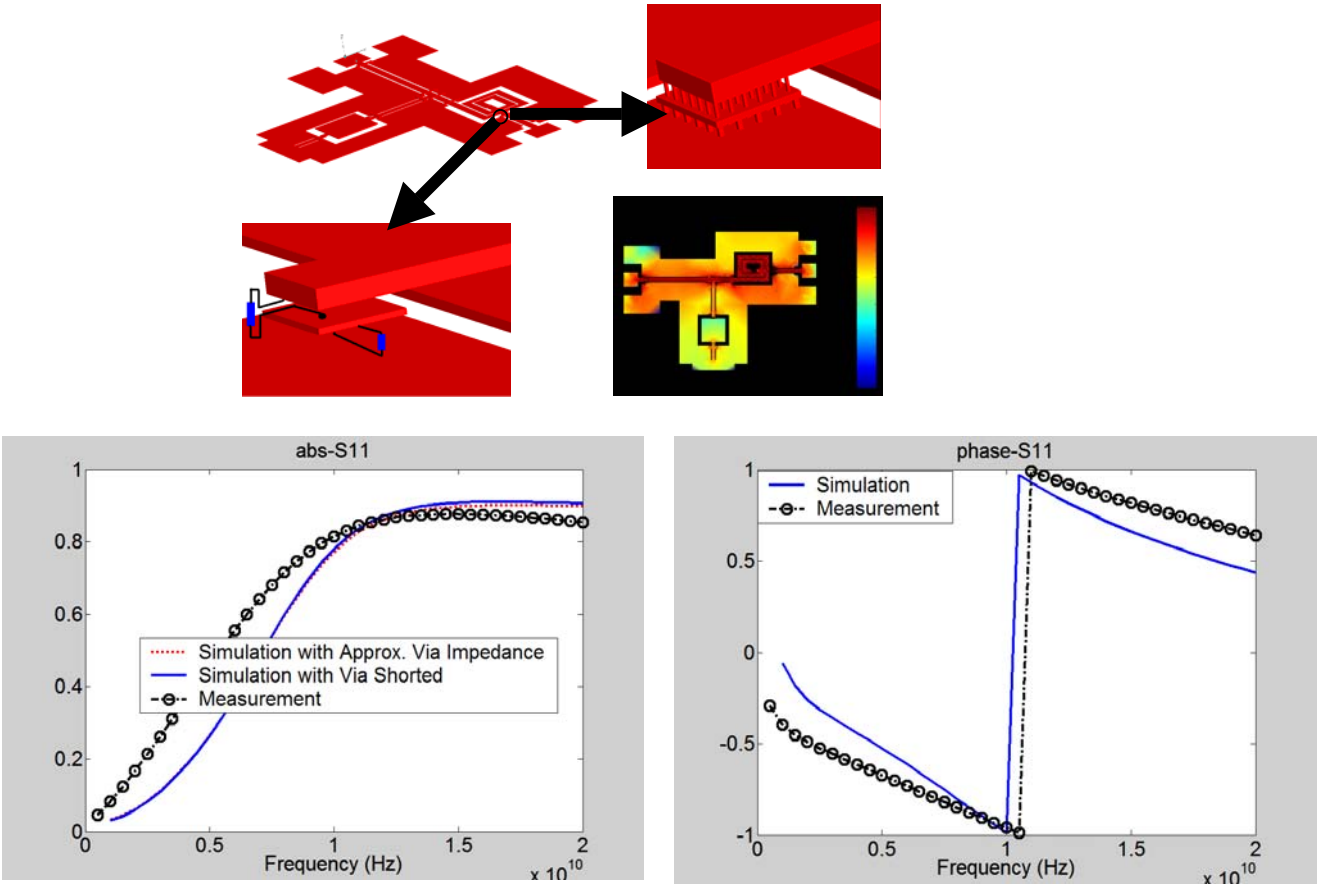

Figure 21: Top: Analog circuit layout, including details of vias and lumped circuit approximations, and current density obtained at 1GHz. Bottom: S-parameters and comparison to measurement.

Finally, the complete power of a surface-based, accelerated MoM solver (PILOT in this case) is shown as in the case of a 4 layer analog sub-circuit that includes a multi-layer inductor, vias, capacitor, coplanar waveguides, and waveguide tees. The entire simulation, completed over the entire frequency band shown in the results, required 15 minutes on a single PC.

7. Discussion

This article presented a review of surface-only MoM formulations starting with a summary of surface equivalence principle examples. The case of conducting media was also discussed in particular. Several critical parts of a real-world, powerful MoM code such as PILOT, such as fast multilevel solvers and frequency sweeps, low-frequency conditioning and preconditioning, numerical quadrature, and parallelization have not been discussed in this article. The main aim was to summarize the power, generalization and completeness of surface formulations as developed by a host of excellent researchers. It should be pointed out that there are certainly instances where hybrid surface-volume formulations, or FEM/FDTD formulations, are better suited owing to conditioning issues. In the final analysis, a truly adaptive hybrid code with all these features as well as time and frequency versions, functioning seamlessly with other multi-physics engines, would be a desirable goal within CEM!

8. Acknowledgements

The authors would like to thank Drs. Dipanjan Gope and Yong Wang, and graduate students Chuanyi Yang, Gong Ouyang, Indranil Chowdhury, James Pingenot, and Todd West who have all contributed to MoM development at the ACE Lab. Funding from DARPA, NSF, SRC, INTEL, ANSOFT, NASA, Lawrence Livermore National Labs, and the University of Washington is gratefully acknowledged.

9. Bibliography

The following is a set of excellent papers, but is by no means exhaustive.

[1] R. F. Harrington, *Field Computation by Moment Methods*, Krieger publishing Co., Malabar, Florida, pp. 71-72,1982.

[2] S. M. Rao, D. R. Wilton and A. W. Glisson, “Electromagnetic scattering by surfaces of arbitrary shape,” *IEEE Trans. on Antennas and Propagation*, vol. 30, pp. 409-418, May 1982.

[3] D. Wilton, S. Rao, A. Glisson, D. Schaubert, O. Al-Bundak and C. Butler, “Potential integrals for uniform and linear source distributions on polygonal and polyhedral

domains, ”*IEEE Trans. on Antennas and Propagation*, vol. 32(3), pp. 276 -281, Mar. 1984.

[4] J.S. Zhao and W.C. Chew, “Integral equation solution of Maxwell's equations from zero frequency to microwave frequencies,” *IEEE Trans. on Antennas and Propagation* vol. 48(10), pp. 1635-1645, Oct. 2000.

[5] Umashankar, A.Taflove and S.Rao, “Electromagnetic scattering by arbitrary shaped three-dimensional homogeneous lossy dielectric objects,” *IEEE Trans. on Antennas and Propagation*, vol. 34(6), pp. 758-766, Jun 1986.

[6] A.J. Poggio, E.K. Miller, Y. Chang, R.F. Harrington, T.K Wu and L.L. Tsai. PMCHWT combined integral equation formulation named after the contributors, 1973-1977. Original collective work.

[7] B.M. Kolundjiza, “Electromagnetic modeling of composite metallic and dielectric structures,” *IEEE Trans. On Microwave Theory and Tech.* vol. 47(7), pp. 1021-1032, Jul. 1999.

[8] P.M. Goggans, A.A. Kishk and A.W. Glisson, “Scattering from conductors coated with materials of arbitrary thickness,” *IEEE Trans. Of Antennas and Propagation.* vol. 40(1), pp. 108-112, Jan. 1992.

[9] S. Chakraborty and V.Jandhyala, “Evaluation of Green’s Function Integrals in Conducting Media,” *IEEE Trans. on Antennas and Propagation*, vol. 52(12), pp. 3357-3363, Dec 2004.

[10] T.K Sarkar, E. Arvas,.S. Ponnapalli, " Electromagnetic Scattering From Dielectric Bodies,”*IEEE Trans. on Antennas and Propagation*, vol. 37(5),pp. 673 – 676, May 1989.

[11] T.K. Wu and L.L.Tsai, “Scattering from arbitrarily-shape lossy dielectric body of revolution,” Radio Sci. , vol. 12(5), pp. 709-718, 1977.

[12] A. E. Ruehli, “Equivalent circuit models for three-dimensional multiconductor systems,” *IEEE Trans. Microwave Theory and Techniques*, vol. 22(3), pp. 216-221, March 1974.

[13] J. Jin, “The Finite Element Method in Electromagnetics,” *New York: John Wiley & Sons*, 1993.

[14] A. Taflove, “Computational Electrodynamics: The Finite-Difference Time-Domain Method,” *Boston Artech House*, 1995.

[15] T. Sarkar , S. Rao, A. Djordjevic, “Electromagnetic scattering and radiation from finite microstrip structures,” *IEEE Trans. on Microwave Theory and Techniques*, vol. 38(11), pp. 1568 – 1575, Nov. 1990.

[16] D. Schaubert, D. Wilton, A. Glisson, “A tetrahedral modeling method for electromagnetic scattering by arbitrarily shaped inhomogeneous dielectric bodies,” *IEEE Trans. on Antennas and Propagations*, vol. 32(1), pp. 77-85, Jan 1984.

[17] W.C. Chew, J.M. Jin, E. Michielssen and J. Song, “*Fast Efficient Algorithms in Computational Electromagnetics*,” Artech House, Boston, London 2001.

[18] A. W. Glisson, “Electromagnetic scattering by arbitrarily shaped surfaces with impedance boundary conditions,” *Radio Science*, vol. 27(6), pp. 935-943, Nov. 1992.

[19] S. Chen, J. S. Zhao, and W. C. Chew, “ Analyzing low-frequency electromagnetic scattering from a composite object,” *IEEE Trans. on Geoscience and Remote Sensing*, vol. 40(2), pp. 426-433 , Feb. 2002.

[20] J.M Putnam and , L.N. Medgyesi-Mitschang, “Combined field integral equation formulation for inhomogeneous two and three-dimensional bodies: the junction problem,” *IEEE Trans. on Antennas and Propagation*, vol. 39(5), pp. 667 – 672, May 1991.

[21] J.R.Mautz and R.F. Harrington, “A combined-source solution for radiation and scattering from a perfectly conducting body,” *IEEE Trans. on Antennas and Propagation*, vol.27, pp-445-454, 1979.

[22] T.K Sarkar, B. Kolundjiza, A.R. Djordjevic and M. Salazar-Palma, “Accurate modeling of frequency responses of multiple planes ingigahertz packages and boards,” *IEEE Conference on EPEP*, pp. 59-62, 2000.

[23] J.Wang, J. Tausch, and J. White, “A wide frequency range surface integral formulation for 3-D RLC extraction,” in *Dig. Technical Papers Int. Conf. Computer-Aided Design*, pp. 453–457,Nov. 1999.

[24] A. W. Glisson, “Electromagnetic scattering by arbitrarily shaped surfaces with impedance boundary conditions,” *Radio Sci.*, vol. 27(6), pp. 935–943, Nov. 1992.

[25] A**.** W.Glisson,"An integral equation for electromagnetic scattering by homogeneous dielectric bodies", *IEEE Trans. on Antennas and Propagation*, vol. 32, pp. 173-175, Feb. 1984.

[26] T.K.Sarkar, E. Arvas and S. Ponnapalli, "Electromagnetic scattering from dielectric bodies," *IEEE Trans. on Antennas and Propagation*, vol. 37(5), pp. 673-676, May 1989.

[27] R. Mittra, and D. R. Wilton, "A numerical approach to the determination of electromagnetic scattering characteristics of perfect conductors," *Proceedings of the IEEE*, vol. 57(11), pp.2064 – 2065, Nov. 1969.

[28] C.C. Lu and W.C. Chew, "A coupled surface-volume integral equation approach for the calculation of electromagnetic scattering from composite metallic and material targets," *IEEE Transactions on Antennas and Propagation*, vol. 48(12), pp. 1866 – 1868, Dec. 2000.

[29] T.E. Van Deventer.; P.B. Katehi and A.C. Cangellaris, "An integral equation method for the evaluation of conductor and dielectric losses in high-frequency interconnects," *IEEE Transactions on Microwave Theory and Techniques*, vol. 37(12), pp.1964 – 1972, Dec 1989.